# Uncertainty Analysis of Risk Estimation in Human Health Risk Assessment of Black Soot Pollution Exposure in Warri Metropolis, Nigeria

**S.P. Oghenerhoro[1], O. Ogoegbulem[2], G.S. Nduka[3], C. Achudume[4], T.E. Eyetan[5], B.I. Akpobroka[6]**

**[1]Department of Environmental Management and Toxicology, Dennis Osadebay University, Asaba, Nigeria**

**[2,3,6]Department of Mathematics, Dennis Osadebay University, Asaba, Nigeria**

**[4]Department of Computer Science and Mathematics, Evangel University, Akaeze, Ebonyi State, Nigeria**

**[5]Department of Geography, Dennis Osadebay University Asaba, Nigeria**

**DOI: https://doi.org/10.51584/IJRIAS.2026.11070111**

**Received: 22 July 2026; Accepted: 27 July 2026; Published: 08 August 2026**

## ABSTRACT

This study analyses uncertainty associated with environmental health risk extraction from black soot pollution on the exposed population in Warri metropolis, using the USEPA (1989) environmental health risk assessment equation approach. The study was aimed at providing informed confidence in risk assessment for the exposed population to black soot pollution and to develop a "comfort level" with the approach. The aim was achieved through the adoption of point estimate, parametric variance propagation, and a ninety-five percent (95%) confidence interval-based context. In this context, three hundred and eighty-five (385) samples were collected for each input parameter. A risk extract was obtained using the point estimate approach. However, a nominal range sensitivity analysis of the model inputs identified exposure duration as the most influential risk driver, with a swing weight of $3.4\times10^{-1}$, whereas human body mass had the least influence, with a swing weight of $3.7\times10^{-6}$. Input parametric probability distribution functions (PDFs) for the propagation were developed using sample statistics and graphics, while the selections were based on certain probability density function models. To effectively utilize the law of parametric uncertainties propagation for the study, the complex multiplicative equation was transformed into an additive functional equation using a logarithmic transformation approach. Also, the log mean and variances of input parameters were obtained using logarithmic distribution algorithms, while the model's uncertainty was propagated as the "root-sum-of-squares" of input log variances to be 2.7. Consequently, the estimated risk was bounded by a 95% confidence interval of $3.7 \times 10^{-2}$ to $3.3 \times 10^{-1}$, with the lower and upper confidence limits determined using the quotient and product of the geometric mean and the square of the geometric standard deviation, respectively. The estimated risk values indicate that although the non-carcinogenic risk remains below the regulatory threshold (HI < 1), prolonged exposure to black soot may still constitute a potential public health concern, particularly for vulnerable populations such as children, the elderly, and individuals with pre-existing respiratory conditions.

**Keywords:** Risk analysis, Human health uncertainty, Model Equation, Pollution exposure

## INTRODUCTION

Globally, Uncertainty analysis has been identified as an essential element of a complete environmental risk analysis on human exposure to pollutants [1, 2]**.** It is, however, imperative that knowledge and reliable methods to deal with uncertainty and variability are also essential for transparency and trust in the risk extraction process. It was opined that transparency is an important factor in the risk management process and has a potential effect on how the risk of environmental pollution is perceived [3,4]

In addition, an appropriate treatment of variability and uncertainty in risk assessment is essential as a basis for decision-making, because of inherent uncertainties in environmental risk models or estimates [5, 6].

However, researchers, the scientific community, and decision- makers also ascertain the fact that to navigate the dynamics of the risk management process properly, the techniques of environmental health risk extraction from ecological pollution scenarios must be capable of building the level of confidence in required results [7-10]. These abstractions become imperative for environmental pollution risk extraction studies because of acknowledged inherent uncertainties in ecological risk extraction models or algorithm formulations, and results that force decision-makers to judge how probable it is that risks will be over-estimated or under-estimated for every exposed person in an environmental pollution scenario [11, 12].

It is important to note that uncertainties in models or algorithms and results are from incommensurability between the real and mathematical world, and the United States Environmental Protection Agency identified three broad sources of uncertainties in the environmental risk analysis context [13-16]. They are categorized into model, parametric, and scenario uncertainty. Primarily, sources of uncertainty are associated with errors in the model’s mathematical construction or uncertainty in the model’s parameters. While parametric uncertainty arises and manifests itself in a variety of ways, which are not limited to measurement uncertainty, variability in time and space, use of appropriate parametric values, and correlations.

However**,** uncertainty analysis as the science of characterization and reduction of uncertainties, in both models and real-world applications, is highly noted [17, 18]. There are two methods of uncertainty analysis: analytical and numerical methods. Analytical methods are variance propagation and moment matching techniques, while numerical methods are Monte Carlo simulation techniques and deterministic uncertainty analysis. The numerical methods combine model parametric inputs, uncertainty, and variability to produce model output uncertainty through simulation, while the analytical methods employ input uncertainties and variability to produce the true but unknown value of output through probability statistics, such as mean, standard deviation, and variance.

Mathematical ability to translate models' or algorithms’ inabilities to provide an exact description or explanation of scenarios of events that occurred as a result of lack of knowledge and variability into a probability distribution or function (PDF) is expressed with key notes [19, 20].

Researchers also emphasize the use of the Probability density function (PDF) to describe uncertainty in the estimate of a quantity that is a fixed constant whose value is not exactly known, or it can be used to describe inherent variability [21, 22]. In correlation to these opinions, aleatory uncertainty, which arises from spatial, temporal, and population variability in nature, could be represented by a function that represents the relative frequency with which different values of a parameter occur [23, 24]. It was also emphasized that uncertainty due to the limitation of knowledge can be represented by a mathematical probabilistic distribution function [25, 26]. Accordingly, moments are used to describe the shape of a probability distribution and thereby the variability [27, 28]._Although probability theory has been accepted as a suitable tool to describe parametric uncertainty. Other complementary methods, such as interval analyses and fuzzy logic, have also been ascertained to incorporate uncertainty about the parameters; that uncertainty about the parameters is normally incorporated by using probabilistic sensitivity analysis.

## METHODOLOGY

The methodology involves risk extraction using point estimate analysis; sensitivity analysis of the US EPA (2009) environmental risk analysis model’s parameters; the determination of probability distributions for input parameters; development of probability distribution functions (PDFs) for the input parameters, parametric propagation of the uncertainties through the model, and analysis of the probability distribution of the risk estimates. The maximum likelihood estimate at a 95% Confidence interval for the propagated model’s geometric mean was employed to determine the true but unknown value of risk for the exposed population to the black soot pollution scenario.

### Risk Extraction

The risk was extracted by applying the analytical point estimate methodology, using the reconstructed US environmental risk analysis equation for the obtained input parameters from three hundred and eighty - three sampled stations across Warri metropolis. Focusing on the inhalation exposure pathway as reconstructed in Equation 3, from the exposure dose intake rate $(D_T)$, hazard quotient $(HQ)$, and hazard index $(Hi)$ as documented. In this regard, the issues of risk and its effects cut across various aspects of human dealings, which need dire attention [29-34]. The input parameters are: ambient concentration of blacksoot $(C_b)$, Inhalation rate of the exposed person $(P_r)$, Duration of exposure $(E_d)$, Body mass of the exposed person $(B_m)$ and environmental reference dose concentration $(Rf_c)$

$$D_T = \frac{C_b \times P_r \times E_d \times n \times a_{(inhalation)}}{B_M} \tag{1}$$

where; $D_T$ =Dose intake (mg/kg/day), $(C_b)$ = ambient concentration of black soot, $(P_r)$ = Inhalation rate of the exposed person, $(E_d)$= Duration of exposure, $(B_m)$= Body mass of exposed person, $n$: Mean number of events per day (events/day); $a_{(inha)}$: Uptake Fraction (inhalation) (dimensionless), $a_{(inha)} = 1:(100\%)$. Based on the risk point estimate, the non-carcinogenic risk index was expressed in terms of dose intake using the Screening Index and Hazard Quotient approaches, as shown in Equation (2), and subsequently reconstructed as Equation (3).

$$\text{SI} = \frac{D_T}{Rf_c} \tag{2}$$

where $Rf_c$ is the environmental reference dose (or reference concentration).

$$HI = \frac{C_b P_r E_d n a_{inhalation}}{BMR_{fc}} \tag{3}$$

where $Hi$ denotes the Hazard Index, $C_b$ is the concentration of the pollutant, $P_r$ represents the pulmonary respiration rate, $E_d$ is the exposure duration, $na_{inhalation}$ denotes the exposure frequency, (inhalation) is the inhalation absorption factor, $BM$ represents the body mass, and $Rf_c$ denotes the environmental reference dose (reference concentration).

Taken $n = 1$ and $a = 1$. Then (3) becomes (4), which is used for the point estimate analysis.

$$RI = \frac{C_b P_r E_d}{BMR_{fc}} \tag{4}$$

However, the sample means presented in Table 1.0 used for the point estimate were obtained from three hundred and eighty-five samples using the computer software SPSS version 25. A risk index of $4.8 \times 10^{-1}$ was extracted from the black pollution scenario on the exposed population, using the point estimate methodology.

The **Risk Index** $(RI)$ is given by

$$RI = \frac{\left(\frac{C_b P_r E_d}{BM}\right)}{Rf_c} = \frac{C_b P_r E_d}{BM \times Rf_c}$$

where $RI$ denotes the Risk Index, $C_b$ is the concentration of the pollutant, $P_r$ represents the pulmonary respiration rate, $E_d$ is the exposure duration, $BM$ denotes the body mass, and $Rf_c$ is the environmental reference dose (reference concentration).

The sample means presented in Table 1 were used as point estimates in the risk assessment and were obtained from a total of 385 samples analyzed using the Statistical Package for the Social Sciences (SPSS) Version 25. Using the point estimate approach, a Risk Index value of $4.8\times10^{-1}$ was obtained for the exposed population under the black soot pollution scenario. This result indicates a moderate level of potential health risk associated with exposure to black soot pollutants within the study area.

**Sensitivity analysis**

A nominal range sensitivity analysis method was adopted, as demonstrated in previous studies [35, 36]. In this context, each of the input parameters was parameter were varied one at a time, while ranges of risks were extracted by keeping the remaining parameters at their approximate median. Having obtained 5% lower limits and 95% upper limits of the parameter distribution, the following ranges of risks, as tabulated in Table 2.0, were obtained and ranked according to their importance in Table 3.0, using the swing weight approach.

**Development and selection of inputs Probability distribution functions (PDFs)**

Statistical graphics and summaries that fit the input parameters were used to synthesize the probabilistic simulations of 385 values of each obtained sample across the metropolis, to develop parametric probability distribution functions (PDFs). While, the selections were based on probability density function models as presented in Table 1.0

Table 1.0. Assigned Probability Distribution Functions (PDFs) for Model Inputs

| **Model Input** | **PDF** | **Parameter 1** | **Parameter 2** | **Parameter 3** |
|---|---|---|---|---|
| $BM$ | Log-Triangle | ln(Min) | ln(Mode) | ln(Max) |
| $P_r$ | Log-Uniform | ln(Min) | ln(Max) | – |
| $C_b$ | Log-Normal | $\mu_{ln}$ | $\sigma_{ln}$ | – |
| $E_d$ | Log-Triangle | ln(Min) | ln(Mode) | ln(Max) |
| $Rf_c$ | Log-Triangle | ln(Min) | ln(Mode) | ln(Max) |

**Analytical propagation of input uncertainties**

This methodology employed input uncertainties and variability to produce the true but unknown value of the output through probability statistics, such as mean, mode, standard deviation, and variance, and PDF algorithms. Input statistics were obtained as in Table 2.0, using SPSS Version 25.0. However, the analytical PDF algorithms presented in equations 6, 7, 8, 9, and 10 were obtained in accordance with the developed probability distribution functions (PDFs) in section 2.3. For lognormal- distributed parameters, log means and variances were analytically obtained by equations (6) and (7), respectively. While the log mean and variance of log-uniformity distributed parameters were calculated with equations (8) and (9), respectively. In addition, Equations (10) and (11) were employed to determine the means and variances of log-triangular distributed parameters in accordance with established methods reported in the literature. Means and variances of the logarithmic distributions are as tabulated in Table 5.0, and were estimated based on obtained parametric statistics: the arithmetic mean, standard deviation, and variances of untransformed sample data.

ISSN No. 2454-6194 | DOI: 10.51584/IJRIAS |Volume XI Issue VII July 2026

$$\mu_{C_b} = \ln\left(\frac{\bar{x}}{\sqrt{1+\left(\frac{SD}{\bar{x}}\right)^2}}\right) \quad (6)$$

$$\delta^2_{C_b} = \ln\left(\frac{\bar{x}^2 + SD^2}{\bar{x}^2}\right) \quad (7)$$

$$\mu_P = \frac{\ln(\min) + \ln(\max)}{2} \quad (8)$$

$$\delta_P = \frac{\ln\left(\frac{\max}{\min}\right)}{\sqrt{12}} \quad (9)$$

$$\mu_{TD} = \frac{\ln(M_0) + \ln(\max) + \ln(\min)}{3} \quad (10)$$

$$\sigma_{TD} = \sqrt{\frac{\left\{\begin{array}{l}[\ln(\min)]^2 + [\ln(\max)]^2 + [\ln(M_0)]^2 \\ -\ln(M_0)[\ln(\min) + \ln(\max)] \\ -\ln(\min)\ln(\max)\end{array}\right\}}{18}} \quad (11)$$

**Uncertainty Propagation through the Extractive Model**

According to the Atomic Energy Control Board (AECB, 1985), variance is a measure of parametric uncertainty, and model uncertainty is the summation of the model's input variances. This is in correlation with the law of uncertainty propagation. Consequently, the uncertainty in the risk extract was $\left(S_{RI}\right)^2 = \sum_{i=1}^{P} S_i^{\,2}$ , where; $p$ , is the model's input parameters.

Observably, the risk extraction equation is a complex multiplicative form of equation that needs normality in accordance with the probabilistic concept of normality to obtain a summation effect. This was achieved using a logarithmic transformation technique documented in the literature. The technique has been successfully applied across diverse fields of research, with the logarithmic distribution parameters (mean and variance on the logarithmic scale) being readily interpretable in terms of multiplicative factors, thereby making the transformed parameters intuitive for analysis. Consequently, the multiplicative relationship was converted into an additive one by taking the logarithm of both sides of Equation (4), resulting in Equation (12).

$$In(RI) = In\left(\frac{P_r C_r V_r}{B_m R_{fc}}\right) \quad (12)$$

In the context of this study, the law of uncertainty propagation, commonly called the "root-sum-of-squares" or "RSS" method, was reconstructed with equations (13) and (14)

$$\left.\begin{array}{l}\delta^2_{(RI)} = \left(\frac{\partial HI}{\partial C_b}\right)^2 \delta^2_{(C_b)} + \left(\frac{\partial HI}{\partial P_r}\right)^2 \delta^2_{(P_r)} + \left(\frac{\partial HI}{\partial V_y}\right)^2 \delta^2_{(V_y)} \\ \quad + \left(\frac{\partial HI}{\partial BM}\right)^2 \delta^2_{(BM)} + \left(\frac{\partial HI}{\partial R_{(fc)}}\right)^2 \delta^2_{(R_{(fc)})}\end{array}\right\} \quad (13)$$

INTERNATIONAL JOURNAL OF RESEARCH AND INNOVATION IN APPLIED SCIENCE (IJRIAS)
ISSN No. 2454-6194 | DOI: 10.51584/IJRIAS |Volume XI Issue VII July 2026

$$\delta_{(RI)} = \sqrt{\begin{Bmatrix} \left(\frac{\partial HI}{\partial C_b}\right)^2 \delta^2_{(C_b)} + \left(\frac{\partial HI}{\partial P_r}\right)^2 \delta^2_{(P_r)} + \left(\frac{\partial HI}{\partial V_y}\right)^2 \delta^2_{(V_y)} \\ + \left(\frac{\partial HI}{\partial BM}\right)^2 \delta^2_{(BM)} + \left(\frac{\partial HI}{\partial R_{(fc)}}\right)^2 \delta^2_{(R_{(fc)})} \end{Bmatrix}} \tag{14}$$

For uncertainty addition and subtraction:

$$\frac{\partial HI}{\partial C_b}, \frac{\partial HI}{\partial P_r}, \frac{\partial HI}{\partial BM}, \frac{\partial HI}{\partial R_{fc}}, \frac{\partial HI}{\partial V_y} \rightarrow \pm 1$$

Therefore, uncertainty in the extracted risk is:

$$\delta_{(RI)} = \sqrt{\delta^2_{(C_b)} + \delta^2_{(P_r)} + \delta^2_{(E_d)} + \delta^2_{(R_{(fc)})} - \delta^2_{(BM)}} \tag{15}$$

**Confidence Interval development for extracted risk**

Confidence in the extracted risk was evaluated using established statistical approaches reported in the literature. Accordingly, approximately 95.4% of the extracted risk values were bounded by the quotient of the geometric mean $\left(\mu_g\right)$, providing a measure of confidence in the estimated risk and the square of the geometric standard deviation$\left(\delta_g{}^2\right)$ *for the* lower bound $\left(X_5{}^{HI}\right)$, while the product of the geometric mean and the square of the geometric standard deviation is for the upper bound $\left(X_{95}{}^{HI}\right)$ as expressed in equations (16), and (17), respectively. Thus,

$$X^{(RI)}_{(5)} = \frac{\mu_g(RI)}{\delta^2_g(RI)} \tag{16}$$

$$X^{(RI)}_{(95)} = \mu_g(RI)\delta^2_g(RI) \tag{17}$$

where, Sample Geometric Mean: $\mu_g\left(RI\right) = e^{\mu InRI}$ (18)

If $X^{(RI)}_{(5)} = \frac{\mu_g(RI)}{\delta^2_g(RI)}$, $X^{(RI)}_{(95)} = \mu_g(RI)\delta^2_g(RI)$ represent the 5th and 95th percentiles of a lognormal distribution, the statistically correct expressions are

$$X^{(RI)}_{(5)} = \frac{\mu_g(RI)}{\delta_g^{(1.645)(RI)}}, \qquad X^{(RI)}_{(95)} = \mu_g(RI)\delta_g^{(1.645)(RI)} \tag{19}$$

and

$$X^{RI}_{95} = \mu_g(RI)\delta_g^{1.645}(RI),$$

rather than using the square of the geometric standard deviation. The exponent 1.6451.6451.645 corresponds to the $5th$ and $95th$ percentiles of the standard normal distribution and is the standard formulation in environmental and human health risk assessment. If, however, you are following a specific published methodology that uses the square of the geometric standard deviation, then your original Equations (16) and (17) are acceptable.

ISSN No. 2454-6194 | DOI: 10.51584/IJRIAS |Volume XI Issue VII July 2026

However, the logarithmic mean of the risk extract $(RI)$ is expressed as;

$$\mu_{(RI)} = \sum_{(i=1)}^{p} \mu_i \tag{20}$$

$$\mu_{(RI)} = \mu_{(C_b)} + \mu_{(P_r)} + \mu_{(V_y)} - \mu_{(BM)} - \mu_{(R_{(fc)})} \tag{21}$$

Geometric standard deviation ($GSD$); $S_g(RI) = S_{InRI} = e^{(S_{In}RI)}$ (22)

$$X_{(5)}^{(RI)} = \frac{\mu_g(RI)}{\delta_g^{(1.645)(RI)}} = \frac{e^{\mu_{(\ln RI)}}}{e^{1.645\delta_{(\ln RI)}}} = \frac{e^{-2.24}}{e^{1.70}} = \frac{0.11}{3.00} = 0.037 = 3.7\times10^{-2}$$

$$\left.\begin{aligned} X_{(95)}^{(RI)} &= \mu_g(RI)\delta_g^{(1.645)(RI)} = e^{\mu_{(\ln RI)}} e^{1.645\delta_{(\ln RI)}} \\ &= e^{-2.24}\times e^{1.70} = 0.11\times3.00 \\ &= 0.33 = 3.3\times10^{-1} \end{aligned}\right\}$$

## RESULTS AND DISCUSSION

A risk index of $4.8\times10^{-1}$ was extracted from the black pollution scenario on the metropolitan exposed population, using the point estimate methodology. Notably, the point estimate does not incorporate explicit estimates of uncertainty, which may lead to incorrect decisions based on a risk estimate that is either grossly overestimated or associated with high and disproportionate amounts of uncertainty. Hence, it was imperative to perform an uncertainty analysis in this study to quantify the degree of confidence about the risk estimate.

Table 2. Model's Inputs Parametric Statistics

| **Model Inputs** | **No. Sample** | **Min** | **Median** | **Mode** | **Max** | $\bar{x}$ | **SD** | **Variance** |
|---|---|---|---|---|---|---|---|---|
| $C_b$ | 385 | 1.00 | 27.0 | 26 | 36.0 | 25.12 | 6.35 | 40.36 |
| $P_r$ | 385 | 11.30 | 336.0 | 395 | 547.20 | 326.9 | 108.37 | 11744.79 |
| $B_m$ | 385 | 7.8 | 60.2 | 70 | 91.00 | 56.34 | 19.50 | 381.546 |
| $E_d$ | 385 | 8.8 | 4.2 | 4.2 | 18.9 | 4.9 | 2.7 | 7.7 |
| $Rf_c$ | 385 | 25.0 | 25.0 | 25 | 25.0 | 25.0 | 0.00 | 0.00 |

**Point estimate**

Table 3.0 Means of Input Parameters

| Parameter | Mean | Unit | Symbol |
|---|---|---|---|
| Body weight | 56.3 | $Kg$ | $BM$ |
| Pulmonary vent rate | 5.5 | $m^3h^{(-1)}$ | $P_r$ |

ISSN No. 2454-6194 | DOI: 10.51584/IJRIAS |Volume XI Issue VII July 2026

| | | | |
|---|---|---|---|
| Exposure duration | 4.9 | $Hr$ | $E_d$ |
| Blacksoot concentration | 25.0 | $\mu gm^{(-3)}$ | $C_b$ |
| Reference concentration | 25.0 | $\mu gm^{(-3)}h^{(-1)}$ | $Rf_c$ |

**Sensitivity analysis**

Table 4. Nominal Range Sensitivity Analysis

| Parameter | Parameter Range | | | Risk Extracts | |
|---|---|---|---|---|---|
| | Lower | Medium | Upper | Low | High |
| $BM$ | 45.00 | 65.50 | 95.50 | $6.5 \times 10^{-5}$ | $1.3 \times 10^{-3}$ |
| $P_r$ | 0.01 | 3.70 | 5.70 | $2.5 \times 10^{-6}$ | $1.5 \times 10^{-3}$ |
| $C_b$ | 1.00 | 26.00 | 36.00 | $3.6 \times 10^{-5}$ | $1.2 \times 10^{-3}$ |
| $E_d$ | 0.88 | 2.76 | 5.66 | $1.2 \times 10^{-5}$ | $3.4 \times 10^{1}$ |
| $Rf_c$ | 15.00 | 25.00 | 36.00 | $6.8 \times 10^{-4}$ | $1.6 \times 10^{-3}$ |

Table 5. Parametric Ranking by Swing weight method

| Rank | Parameter | **Swing weight** |
|---|---|---|
| 1 | $E_d$ | $(3.4 \times 10^{-1})$ |
| 2 | $P_r$ | $(2.5 \times 10^{-1})$ |
| 3 | $C_b$ | $(2.23 \times 10^{-1})$ |
| 4 | $Rf_c$ | $(1.13 \times 10^{-1})$ |
| 5 | $BM$ | $(3.7 \times 10^{-6})$ |

Three levels of parameter importance appear to emerge from the sensitivity analysis results in Tables 4.0 and 5.0. The duration of the exposed population $(E_d)$ and Pulmonary vent rate (intake rate) $(P_r)$ show clearly a greater influence on the risk estimate, while the concentration of black soot $(C_b)$ and Reference concentration $(Rf_c)$ form the next level of importance. However, body mass $(BM)$ has a moderate influence on the risk. From these results, most of the effort in the study was on quantifying or propagating the uncertainty due to the duration of exposure, population, intake rate, and concentration. However, other groups were also quantified. Also, from the chart in Figure 1.0, the duration of the exposed population $(E_d)$ has a greater influence of 3.4 as compared to the pulmonary vent rate (intake rate $(P_r)$, concentration of black soot $(C_b)$, and Reference concentration $(Rf_c)$ and body mass), $(BM)$ with respective influences of 2.5, 2.2, and 1.1, respectively.

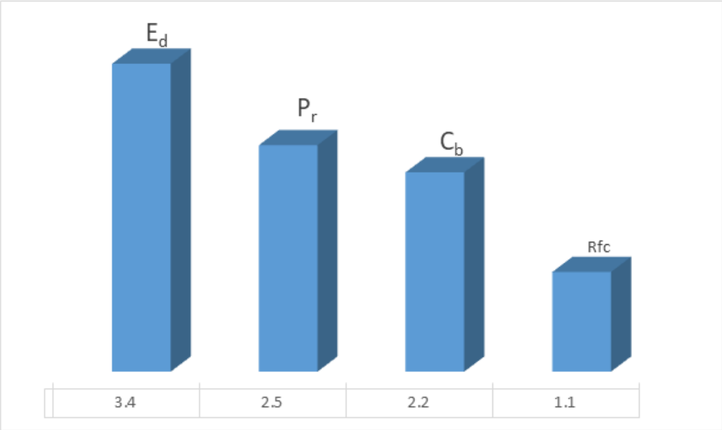


Figure 1.0 Swing Weights of Model's Input Parameters

Considering the parametric uncertainty level, the environmental concentration of black soot and body mass of the exposed population in the metropolis have a greater percentage of uncertainties than other parametric inputs in the risk extract. They contributed 30.39% each to the overall uncertainty in the risk extract, while the duration of individual exposure contributed the lowest percentage of 2.49%, as obtained in Table 6.0 and Figure 2.0.

Table 6.0. Models' Input Parametric Uncertainty Percentages

| Model Parameters | log-variance $(\delta)$ | Percentage $(\%)$ |
|---|---|---|
| $C_b$ | 1.10 | 30.39 |
| $P_r$ | 0.65 | 17.96 |
| $C_b$ | 1.10 | 30.39 |
| $E_d$ | 0.09 | 2.49 |
| $Rf_c$ | 0.68 | 18.79 |

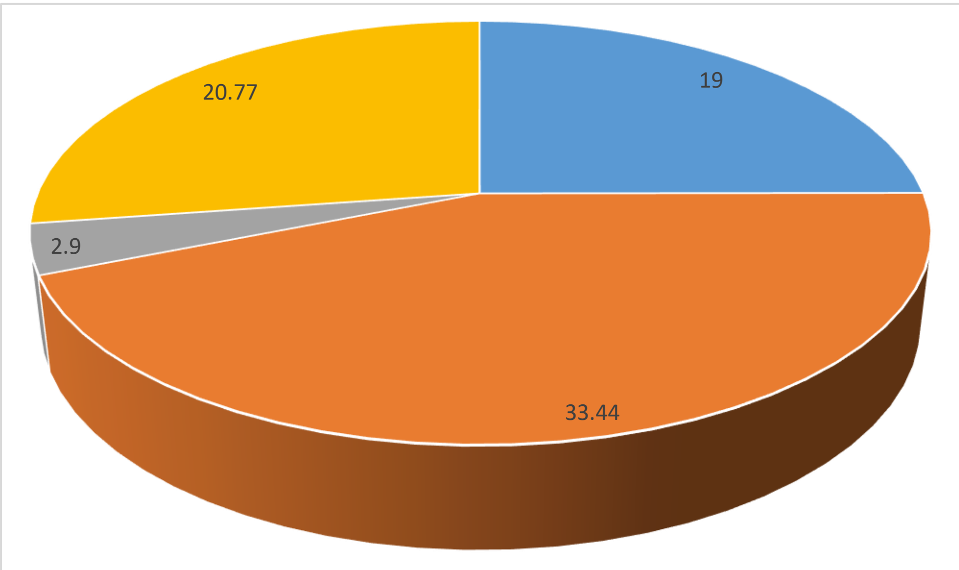


Figure 2.0 Sectoral Model's Inputs Parametric Uncertainties

Imperatively, the uncertainty about a true but unknown distribution of risks per individual exposed to black soot pollution in Warri metropolis $(\delta_{RI})$ was determined as 1.7 using equation

$$\delta_{(RI)} = \sqrt{\delta^2_{(C_b)} + \delta^2_{(P_r)} + \delta^2_{(E_d)} + \delta^2_{(BM)} + \delta^2_{(R_{(fc)})}} \tag{23}$$

While at 95% confidence with inherent uncertainties, the non-carcinogenic health risk extract for exposed persons to black soot pollution within the metropolis lies between $3.7\times10^{-2}$ and $3.3\times10^{-1}$. This describes a range of values within which we can be reasonably sure that the true risk of the black soot pollution scenario on the exposed population actually lies at $3.7\times10^{-2}$ and $3.3\times10^{-1}$. These relatively narrow confidence intervals indicate an effective risk estimate with known precision, and account for uncertainties. It is, however, imperative that risk decisions about environmental risk management interventions for the black soot pollution scenario in Warri metropolis using the equation are made with certainty.

From a public health perspective, the estimated non-carcinogenic risk suggests that the current level of black soot exposure does not indicate an immediate adverse health threat for the average resident. Nevertheless, continuous exposure, especially among highly exposed groups such as commercial drivers, traders, industrial workers, and residents living close to major traffic corridors or illegal refining activities, may increase cumulative health risks. Consequently, sustained air quality monitoring and emission control strategies remain necessary to minimize long-term exposure.

The USEPA exposure model provides a standardized framework for risk estimation; however, exposure characteristics within Warri metropolis may differ from the default assumptions because of local occupational activities, informal refining operations, traffic density, housing ventilation patterns, and socioeconomic conditions. These factors should be considered when interpreting the estimated risks.

The estimated risk levels are comparable to those reported in similar particulate pollution studies conducted in Port Harcourt, Lagos, and other urban centres where black soot episodes have been associated with increased respiratory symptoms and elevated particulate matter concentrations [37-39]. Such comparisons support the consistency of the present findings while highlighting regional differences in exposure characteristics.

## CONCLUSION

Observably, the probabilistic propagation of the black soot pollution's risk drivers (duration of exposed population $(E_d)$, pulmonary vent rate (intake rate) $(P_r)$, concentration of black soot $(C_b)$, Reference concentration $(Rf_c)$, and body mass $(BM)$, with their resultant risk extract at 95% confidence interval) presented a more complete and realistic characterization of the risk extract between $3.7\times10^{-2}$ and $3.3\times10^{-1}$ instead of a single, deterministic point estimate of $4.8\times10^{-1}$. This has offered confidence dynamics in the risk management deliberation process for Warri's black soot pollution scenario using the equation for pollution risk extracts. From the parametric sensitivity analysis results, effort should be more on the duration of exposure of persons, the intake rate, and the concentration of black soot in pollution management decisions. In addition, to reduce uncertainties in pollution risk estimates using the equation, further studies should critically look at measurement and variability uncertainties in the ambient concentration of black soot.

Future studies should complement the quantitative risk assessment with epidemiological investigations, biomonitoring studies, and clinical assessments to establish stronger associations between black soot exposure and adverse health outcomes among residents of Warri metropolis. Such studies would provide additional evidence for environmental health policy and intervention programmes.

## REFERENCES

1. Thelen, A., Zhang, X., Fink, O., Lu, Y., Ghosh, S., Youn, B. D., ... & Hu, Z. (2023). A comprehensive review of digital twin—Part 2: Roles of uncertainty quantification and optimization, battery digital twins, and future perspectives. Structural and Multidisciplinary Optimization, 66(1).
2. Kirzner, I. M. (2024). Uncertainty, discovery, and human action: A study of the entrepreneurial profile in the Misesian system. In Modern Austrian Economics (Vol. 1, pp. 41–64). Routledge.

3. Nahar, N., Hossain, Z., & Mahiuddin, S. (2023). Assessment of the environmental perceptions, attitudes, and awareness of city dwellers regarding sustainable urban environmental management: A case study of Dhaka, Bangladesh. Environment, Development and Sustainability, 25(8), 7503–7531.
4. Ajayi, S. A., Adams, C. A., Dumedah, G., Adebanji, O. A., Ababio-Donkor, A., Ackaah, W., & Kehinde, A. (2023). Public perceptions of vehicular traffic emissions on health risk in Lagos metropolis, Nigeria: A critical survey. Heliyon, 9(5), Article eXXXXX. (Replace with the article number if available.)
5. Badeenezhad, A., Soleimani, H., Shahsavani, S., Parseh, I., Mohammadpour, A., Azadbakht, O., ... & Babakrpur Nalosi, K. (2023). Comprehensive health risk analysis of heavy metal pollution using water quality indices and Monte Carlo simulation in R software. Scientific Reports, 13(1), Article 15817.
6. Wei, R., Chen, C., Kou, M., Liu, Z., Wang, Z., Cai, J., & Tan, W. (2023). Heavy metal concentrations in rice that meet safety standards can still pose a risk to human health. Communications Earth & Environment, 4(1), Article 84.
7. Claxton, K., Sculpher, M., & Drummond, M. (2002). A rational framework for decision-making by the National Institute for Clinical Excellence (NICE). The Lancet, 360, 711–715.
8. Park, Y. S., & Lek, S. (2025). Artificial neural networks (multilayer perceptron) for ecological modeling. In Ecological Model Types (pp. 297–322). Elsevier.
9. El Hajj, M., & Hammoud, J. (2023). Unveiling the influence of artificial intelligence and machine learning on financial markets: A comprehensive analysis of AI applications in trading, risk management, and financial operations. Journal of Risk and Financial Management, 16(10), Article 434.
10. Ali, I., Golgeci, I., & Arslan, A. (2023). Achieving resilience through knowledge management practices and risk management culture in agri-food supply chains. Supply Chain Management: An International Journal, 28(2), 284–299.
11. Flinders, C., Barnhart, B., Morrison, E. B., Anderson, P. D., & Landis, W. G. (2025). Probabilistic approaches for risk assessment and regulatory criteria development: Current applications, gaps, and opportunities. Integrated Environmental Assessment and Management, 21(6), 1281–1292.
12. Mousavi, M. N., Ghalehteimouri, K. J., Hekmatnia, H., Bagheri-Kashkouli, A., & Kahaki, F. (2025). Evaluating sector-based impact of environmental indicators on Iran GHG emissions: A scenario development approach. Environment, Development and Sustainability, 27(9), 20887–20914.
13. Ogwu, M. C., Izah, S. C., Sawyer, W. E., & Amabie, T. (2025). Environmental risk assessment of trace metal pollution: A statistical perspective. Environmental Geochemistry and Health, 47(4), Article 94.
14. Lockie, S., Graham, V., Taylor, B., Baresi, U., Maclean, K., Paxton, G., & Vella, K. (2025). Conceptualizing social risk in relation to climate change and assisted ecosystem adaptation. Risk Analysis, 45(3), 668–681.
15. Ma, F., Cao, J., Wang, Y., Vigne, S. A., & Dong, D. (2025). Dissecting climate change risk and financial market instability: Implications for ecological risk management. Risk Analysis, 45(3), 496–522.
16. Pereira, R., Sousa, J. P., Niemeyer, J., Markwiese, J., Andersen, C. P., & Cachada, A. (2026). Ecotoxicological effects and risk assessment of pollutants. In Soil Pollution (pp. 241–270). Academic Press.
17. Fadeeva, E., Rubashevskii, A., Shelmanov, A., Petrakov, S., Li, H., Mubarak, H., Tsymbalov, E., Kuzmin, G., Panchenko, A., Baldwin, T., & Nakov, P. (2024). Fact-checking the output of large language models via token-level uncertainty quantification. In Findings of the Association for Computational Linguistics: ACL 2024 (pp. 9367–9385). Association for Computational Linguistics.
18. Qiu, X., & Miikkulainen, R. (2024). Semantic density: Uncertainty quantification for large language models through confidence measurement in semantic space. Advances in Neural Information Processing Systems, 37, 134507–134533.
19. Mehdiyev, N., Majlatow, M., & Fettke, P. (2025). Quantifying and explaining machine learning uncertainty in predictive process monitoring: An operations research perspective. Annals of Operations Research, 347(2), 991–1030.
20. Sobhanardakani, S., & Hosseini, N. S. (2026). Modeling health risks from urban roadside soil toxic elements using two-dimensional Monte Carlo simulation paired with multiple linear regression. Journal of Environmental Chemical Engineering, 14(2), Article 121843.
21. Keshmiri, E., & Ahmadi, M. M. (2025). Reliability analysis of circular foundations on unsaturated soils using Monte Carlo simulation. Geotechnical and Geological Engineering, 43(2), Article 111.

22. Juodis, A. (2025). This shock is different: Estimation and inference in misspecified two-way fixed effects panel regressions. Econometric Theory, 1–34. (Advance online publication or page range to be updated when assigned to an issue.)
23. Lou, X., Luo, P., & Meng, L. (2025). Geoconformal prediction: A model-agnostic framework for measuring the uncertainty of spatial prediction. Annals of the American Association of Geographers, 115(8), 1971–1998.
24. Wang, K., Shen, C., Li, X., & Lu, J. (2025). Uncertainty quantification for safe and reliable autonomous vehicles: A review of methods and applications. IEEE Transactions on Intelligent Transportation Systems. (Add volume, issue, and page/article number if available.)
25. Bijma, F., Erné, R., Jonker, M., & van der Vaart, A. (2025). An introduction to mathematical statistics. Routledge.
26. Tukeev, D. L., Afanaseva, O. V., & Tulyakov, T. F. (2026). Realization of statistical models based on symmetric unimodal distributions. International Journal of Engineering, 39, 407–419.
27. Jespersen, C. K., Steinhardt, C. L., Somerville, R. S., & Lovell, C. C. (2025). On the significance of rare objects at high redshift: The impact of cosmic variance. The Astrophysical Journal, 982(1), Article 23.
28. Spivak, B., Trood, M., & McEwan, T. (2026). Validation of an actuarial instrument to predict repeat family violence for frontline police: Calibration, discrimination, and classification performance of the VP-SAFvR. Journal of Family Violence, 41(1), 127–139.
29. Okagbue, H. I., Edeki, S. O., & Opanuga, A. A. (2014). A Monte Carlo simulation approach in assessing risk and uncertainty involved in estimating the expected earnings of an organization: A case study in Nigeria. American Journal of Computational and Applied Mathematics, 4(5), 161–166.
30. Chaudhry, S. M., Chen, X. H., Ahmed, R., & Nasir, M. A. (2025). Risk modelling of ESG (environmental, social, and governance), healthcare, and financial sectors. Risk Analysis, 45(3), 477–495.
31. Edeki, S. O., Ogoegbulem, O., Adinya, I., Ezekiel, I. D., & Masood, C. (2025). Dynamical modeling of climate-related financial risk and the interplay of natural disasters, migration, and loan defaults. Journal of Science and Mathematics Letters, 14(2), 250–264.
32. Adewumi, A. J., & Ogundele, O. D. (2024). Hidden hazards in urban soils: A meta-analysis review of global heavy metal contamination (2010–2022), sources, and its ecological and health consequences. Sustainable Environment, 10(1), Article 2293239.
33. Edeki, S. O., Adinya, I., & Ugbebor, O. O. (2014). The effect of stochastic capital reserve on actuarial risk analysis via an integro-differential equation. IAENG International Journal of Applied Mathematics, 44(2).
34. Onyekwere, C. K., Aguwa, O. C., & Obulezi, O. J. (2025). An updated Lindley distribution: Properties, estimation, acceptance sampling, actuarial risk assessment, and applications. Innovation in Statistics and Probability, 1(1), 1–27.
35. Najjar, A., Hamadeh, A., Krause, S., Schepky, A., & Edginton, A. (2024). Global sensitivity analysis of Open Systems Pharmacology Suite physiologically based pharmacokinetic models. CPT: Pharmacometrics & Systems Pharmacology, 13(12), 2052–2067.
36. Li, S., Kong, D., Xu, Y., Gao, W., Kennel, R., & Heldwein, M. L. (2024). A robust model predictive control for dual active bridge converters based on super-twisting observer and sensitivity analysis. IEEE Journal of Emerging and Selected Topics in Power Electronics, 12(5), 4665–4677.
37. Ossai, C. J., Iwegbue, C. M., Tesi, G. O., Olisah, C., Egobueze, F. E., Nwajei, G. E., & Martincigh, B. S. (2021). Distribution, sources and exposure risk of polycyclic aromatic hydrocarbons in soils, and indoor and outdoor dust from Port Harcourt city, Nigeria. Environmental Science: Processes & Impacts, 23(9), 1328-1350.
38. Yakubu, O. H. (2017). Particle (soot) pollution in Port Harcourt Rivers State, Nigeria—double air pollution burden? Understanding and tackling potential environmental public health impacts. Environments, 5(1), 2.
39. Ekhator, O. C., Orish, F. C., Nnadi, E. O., Ogaji, D. S., Isuman, S., & Orisakwe, O. E. (2024). Impact of black soot emissions on public health in Niger Delta, Nigeria: understanding the severity of the problem. Inhalation Toxicology, 36(5), 314-326.